Mobile Ambipolar Domain in Carbon-Nanotube Infrared Emitters

Marcus Freitag,[1,2] Jia Chen,[1] J. Tersoff,[1] James C. Tsang,[1] Qiang Fu,[3] Jie Liu,[3] and Phaedon Avouris[1,*]

[1]*IBM Research Division, T. J. Watson Research Center, Yorktown Heights, New York 10598, USA*

[2]*Carbon Nanotechnologies, Inc., Houston, Texas 77084, USA*

[3]*Department of Chemistry, Duke University, Durham, North Carolina 27708, USA*

(Received 18 March 2004; published 11 August 2004)

We spatially resolve the infrared light emission from ambipolar carbon-nanotube field-effect transistors with long-channel lengths. Electrons and holes are injected from opposite contacts into a single nanotube molecule. The ambipolar domain, where electron and hole currents overlap, forms a microscopic light emitter within the carbon nanotube. We can control its location by varying gate and drain voltages. At high electric fields, additional stationary spots appear due to defect-assisted Zener tunneling or impact ionization. The laterally resolved measurement provides valuable insight into the transistor behavior, complementary to electronic device characteristics.

DOI: 10.1103/PhysRevLett.93.076803 PACS numbers: 73.63.Fg, 72.20.Jv, 78.60.Fi, 78.67.Ch

Carbon nanotubes (CNTs) are quasi-one-dimensional objects with unique electronic properties [1]. They are direct-gap semiconductors and optically active nanostructures [2,3]. Carbon-nanotube field-effect transistors (CNTFETs) [4,5] with ambipolar characteristics [6,7] have been shown to emit infrared (IR) light, making them the first electrically excited single-molecule light sources [8]. The CNT electroluminescence is due to the recombination of electrons and holes that are injected at the opposite contacts into an individual carbon nanotube. No chemical doping to form a *p-n* junction is necessary because a CNTFET with thin Schottky barriers at the source and drain contacts allows the simultaneous injection of electrons and holes. This property gives great flexibility to the design of a light-emitting device, since no particular nanotube section is predetermined to become the recombination area. Here we report spatially resolved measurements of the infrared emission from long-channel CNTFETs. We find that most of the electroluminescence is confined to a small segment of the carbon nanotube that can be controllably positioned by varying the gate voltage. No equivalent for this behavior exists in 3D devices. Most importantly, by monitoring the position, intensity, and shape of the spot of emitted light in the CNTFET as a function of the biasing conditions, we can obtain new direct information on the carrier transport processes within the device.

Carbon nanotubes with lengths on the order of 100 μm and diameters between 1 and 3 nm were grown by chemical vapor deposition on a silicon substrate covered by 100 nm thick SiO_2. The process is similar to that in Ref. [9] with 3 nm Fe nanoparticles as the catalyst and CH_4 as the carbon source. Two electrical contacts are defined by *e*-beam lithography and evaporation of 30 nm of palladium. The silicon substrate acts as a back gate. Conduction in the CNTFET is ambipolar [7,10]. We image the IR emission from the CNTFETs with a liquid nitrogen-cooled HgCdTe detector array mounted on the camera port of an optical microscope. The lateral resolution is diffraction limited at about 2 μm. The nanotube described here is 3 nm in diameter and 50 μm long. We measure its infrared emission at 2 μm (bandpass filter with 80 nm FWHM), on the high-energy side of the emission peak.

Figure 1(b) shows the gate-voltage (V_g) characteristics of the CNTFET in constant current mode with $I_d = 18\ \mu$A. The sweep starts at $V_g = -40$ V (red curve), where the conduction is carried by holes. The ambipolar state around $V_g = -30$ V is characterized by the large negative drain voltage necessary to drive the current. At $V_g = 0$ V the conduction is carried by electrons. The blue curve shows the reverse sweep. Note that a strong hysteresis develops [11,12] that shifts the ambipolar state [minima in Fig. 1(b)] to gate voltages significantly different from the ideal value [7,8] of $V_g = V_d/2$.

Figure 1(a) shows the spatial behavior of the IR emission during the 800-s gate-voltage sweep. Until frame 7 we observe no IR emission because the device is a pure hole conductor. In frame 8 a light spot appears at the drain contact (top), as minority carriers (electrons) are injected at the drain and recombine radiatively with the majority carriers (holes). As the voltage sweep continues, the light near the drain intensifies because more minority carriers are injected, until during frame 9 the emitting spot that marks the ambipolar region in the device, where electrons and holes coexist, leaves the drain contact region and moves into the nanotube channel. Between frames 9 and 19, the gate voltage controls the location of the ambipolar region. Once the spot reaches the source contact (frame 19), the infrared emission is gradually diminished, as the hole current becomes the new minority carrier current and decreases. During the reverse sweep the spot reappears at the source, moves back toward the drain contact, and disappears there.

A strong hysteresis is observed in both the electronic transfer characteristics in Fig. 1(b) and the light emission

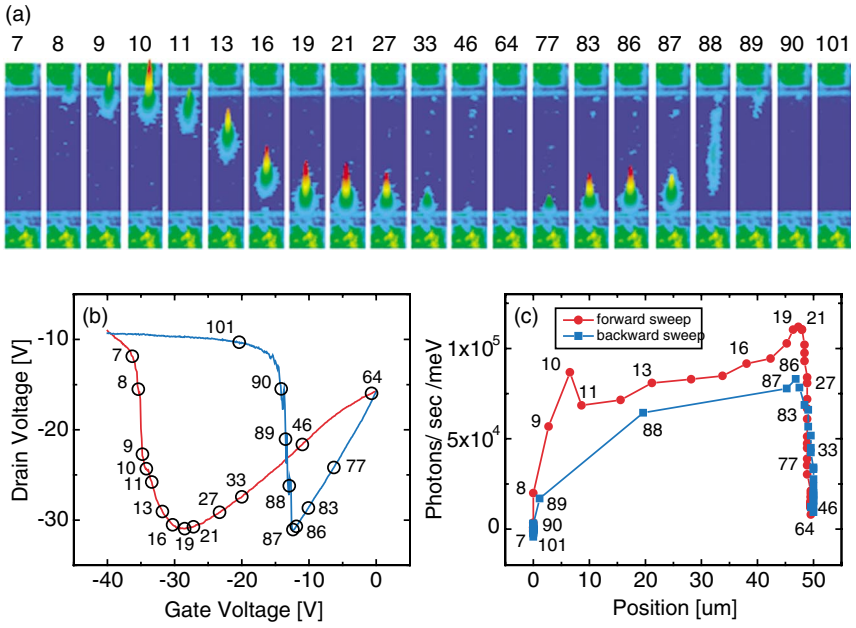

FIG. 1 (color). (a) CNTFET infrared emission during a gate-voltage sweep. (3D plots where x and y are lateral directions on the device and z is the IR intensity.) The light intensity is also color coded. Camera integration for each frame is 6 s. An image of the electrodes is superimposed on all frames to help identify the emitting location. The nanotube (not visible) is aligned vertically between source and drain. (b) Gate-voltage characteristic under which the sequence in (a) was acquired. The measurement is done in constant current mode ($I_d = 18\ \mu$A) by adjusting the drain voltage at the top contact. The source contact is grounded. (c) IR intensity versus position along the carbon nanotube. Numbers in (b) and (c) correlate the data to the frames in (a).

sequence in Fig. 1(a). We can understand this behavior by noting that, because of the high voltages that are used and the nanometer-sized radius of the carbon nanotube, very large electric fields ($\sim 10^7$ V/cm) are generated in the vicinity of the nanotube that can inject charges into the gate insulator [11,12]. The trapped charges act as additional local gate voltages and modify the electrostatics of the device. The behavior of the moving spot could be used to study the process of charge trapping, an interesting topic but beyond the scope of this Letter.

From Fig. 1(a) it is evident that electrons and holes recombine within a distance that is short compared to the tube length. Thus the appearance of a discrete emission spot within the nanotube [e.g., Fig. 1(a), frame 16] means that the current must be all holes at the source and all electrons at the drain. Then the hole current injected at the source must *exactly equal* the electron current injected at the drain, both being $I_d = 18\ \mu$A; these hole and electron currents annihilate where they meet, defining the emission spot. When the two currents are unequal, minority carriers recombine near the point of injections, as in Fig. 1(a), frames 8, 33, and 90.

Both the controllable positioning of the emission spot and the exact balance between electron and hole injection reflect the quasi-1D character of the channel. Transport on this length scale is diffusive, requiring an electric field all along the channel to drive the current. But in this long-channel device, the gate effectively shields the channel from electric fields associated with source or drain voltages, and (on length scales large compared to the gate-oxide thickness) the local potential relative to V_g is a function only of the local charge. Thus when a voltage is applied, charge accumulates in the channel, until the electric field (and chemical-potential gradient) associated with charge gradients along the channel is just sufficient to maintain a uniform steady-state current of I_d at every point. In the regime of midtube light emission, we have an accumulation of holes in the nanotube near the source and electrons near the drain.

The emission spot is the point where the local charge goes to zero (separating electron and hole accumulation regions) and the local potential is V_g. When the applied voltage or current is changed, the charge rearranges to maintain the uniform current, automatically shifting the position of the emission spot. It is this feedback (and analogous feedback in the Schottky-barrier conductance) that allows exactly equal electron and hole injection over a range of voltages. In the limit that nanotube (channel) resistance dominates over contact resistance, the entire bias V_d drops along the carbon nanotube. Thus one can move the ambipolar domain between source and drain by varying V_g between zero and V_d. By examining simple models for the FET behavior, we find that the effect of contact resistance is generally to compress the range of V_g over which the emission spot sweeps from source to drain.

Figure 1(c) shows the infrared emission intensity around $\lambda = 2\ \mu$m versus the position of the emission maximum. Near both contacts, the light intensity varies strongly with the minority carrier currents. On the other hand, when the light source is in the nanotube channel, the intensity is only weakly dependent on the exact position where the recombination occurs, an observation consistent with fixed and equal injected electron and hole currents ($I_e = I_h = 18\ \mu$A). This also implies that the whole device has a position-independent efficiency for radiative recombination. Two apparent exceptions are provided by the areas close to the contacts [Fig. 1(a)] where the intensity is enhanced by $\sim 20\%$ before falling off at the contacts. This is likely due, however, to the

broadening of the spectrum near the contacts where the E field is higher. Since we measure the photons on the high-energy tail of the emission spectrum, the photon count is increased when carriers recombine before thermalizing [13]. The slight increase in measured intensity between frames 11 and 17 coincides with an increase in drain voltage from -26 to -31 V and can also be attributed to the broadening of the spectrum.

We quantify the spatial extent l_r of the recombination region (i.e., the light source) by deconvoluting intensity profiles along the direction of the carbon nanotube with intensity profiles perpendicular to it (Fig. 2). To avoid artificially elongated spots due to the camera integration, we consider only frames where the spot is stationary during the frames immediately before and after. The recombination length l_r varies with the applied bias, e.g., $l_r = 2\ \mu$m in frame 8 ($V_d = -15$ V) and $l_r = 4\ \mu$m in frame 21 ($V_d = -30$ V). If, as in our case, the channel is long compared to l_r, the emission is localized and positionable along the nanotube, while, if the channel is short compared to l_r, the emission is distributed over the whole channel.

Figure 3(a) shows the light emission as a function of drain voltage and position along the carbon nanotube during a drain voltage sweep with $V_g = -5$ V [Fig. 3(b)]. IR emission appears close to the drain contact at a drain voltage of -10 V, when minority carriers

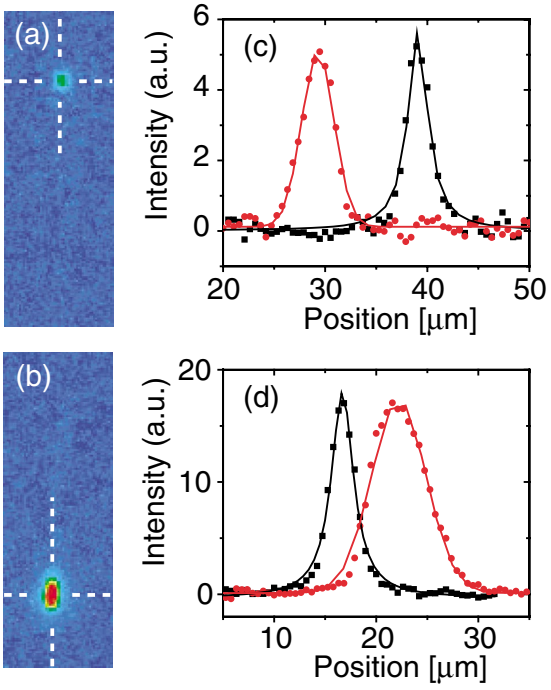

FIG. 2 (color). (a) 2D plot of frame 8 of the sequence in Fig. 1(a). The drain voltage was -15 V. (b) 2D plot of frame 21 of the sequence in Fig. 1(a). The drain voltage was -30 V. (c),(d) Line profiles through the two frames along (red) and perpendicular to (black) the nanotube axis.

(electrons) start to be injected. During the remainder of the forward sweep, the light spot moves within the nanotube channel [Fig. 3(c)] as the injected electron and hole current are matched. Unlike Fig. 1(a), however, the light intensity increases strongly because the current is allowed to change. On the sweep back, the spot returns almost instantly to the drain, where it becomes weaker due to the decreasing injected electron current [Fig. 1(c), blue curve]. The total current, however, remains the same [Fig. 3(b), blue curve between -28 and -12 V]. Figure 3(d) shows the light intensity as a function of the drain voltage during this part of the sweep. Assuming proportionality between photon count and minority carrier current, the light emission is a measure of the Schottky-barrier transparency. The exponential decay of the light intensity is in agreement with the predicted exponential behavior of the leakage current in the off state of an ambipolar CNTFET [7]. In short-channel CNTFETs this current contributes additively to the total current since the minority carriers can reach the opposite contact before recombining. In our long-channel devices, on the other hand, the minority carrier current cannot be measured directly. However, it is responsible for the light emission near the drain electrode.

Finally, we focus on the effect of a large bias on the electroluminescence. Figure 3(e) was acquired during a gate-voltage sweep resembling the one in Fig. 1(b). Source and drain contacts were switched so that the ambipolar region now moves from the bottom contact (the new drain) to the top contact and back. We also increased the current from 18 to 20 μA, a value close to the saturation current for CNTFETs [14], and a substantially larger drain voltage of up to -40 V is now required to drive the current in the ambipolar state [Fig. 3(f)]. Under these conditions additional light spots appear within the carbon nanotube that do not move by changing the gate voltage and therefore appear as horizontal lines in Fig. 3(e). We can resolve at least six spots of stationary electroluminescence of varying intensity. [Two spots are already present at lower voltages in frames 33 to 87 of Fig. 1(a)]. When the CNTFET is in a unipolar state or the moving ambipolar domain is far from such a stationary spot, the current in that nanotube section should be carried by only one type of carrier (electron or hole). On the other hand, both carriers must be present to produce electroluminescence, so we must conclude that minority carriers are generated at the stationary sites. Since the spots appear only under high-field conditions, Zener tunneling or impact ionization from the valence to the conduction band are likely responsible. Zener tunneling tends to be pinned at defects because the tunneling rate is enhanced in the presence of a deep defect or impurity state within the nanotube band gap. Impact ionization will also be enhanced by the high-field conditions present at defect sites [15]. Furthermore, both processes are ex-

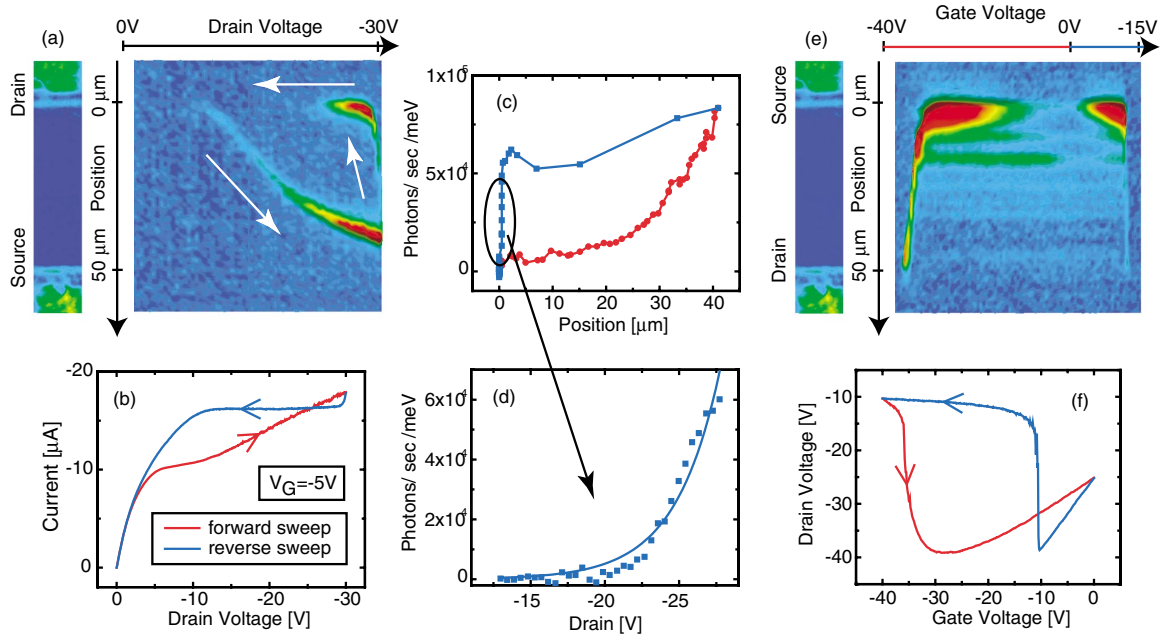

FIG. 3 (color). (a) IR emission as a function of drain voltage and position along the nanotube during a drain voltage sweep at a gate voltage of −5 V. To generate the plot, the localized IR intensity from the nanotube was integrated for each frame of the sequence. (b) Drain voltage sweep during which (a) was taken. (c) IR intensity versus position of the light spot. (d) IR intensity versus drain voltage during the reverse sweep. The solid line is an exponential fit. (e) IR emission as a function of gate voltage and position along the carbon nanotube during a gate-voltage sweep in constant current mode ($I = 20\ \mu$A). (f) Gate-voltage characteristics during which (e) was acquired.

pected to be more prominent in large diameter CNTs with smaller band gaps, such as in our case [16].

In conclusion, the translatable infrared emission from carbon-nanotube field-effect transistors provides a beautiful visual demonstration of the new physics in one-dimensional electronic systems. Abrupt metal-nanotube contacts allow the injection of electrons and holes into an intrinsic, semiconducting channel. When the two types of carriers meet, they form a short ambipolar segment where recombination takes place. By following the recombination spot we determine the location of the interacting boundaries of the electron and hole currents, while the intensity of light provides information about the size of the currents. Local carrier generation sites can also be identified, while analysis of the shape of the light spot provides information on the recombination length. Coupling this technique with detailed simulations should lead to an unprecedented understanding of the transistor action.

We thank V. Perebeinos and J. Appenzeller for valuable discussions, and B. Ek and M. Kinoshita for their help in setting up the experiment. We would also like to acknowledge J. Misewich and R. Martel with whom the early work on this subject was performed. J. Liu acknowledges ARO (DAAD19-00-1-0548) and Dupont for support.

*Electronic address: avouris@us.ibm.com

[1] *Carbon Nanotubes*, edited by M. S. Dresselhaus, G. Dresselhaus, and Ph. Avouris (Springer Verlag, Berlin, 2000).
[2] S. M. Bachilo *et al.*, Science **298**, 2361 (2002).
[3] T. Hertel, R. Fasel, and G. Moos, Appl. Phys. A **75**, 449 (2002).
[4] Phaedon Avouris *et al.*, Proc. IEEE **91**, 1772 (2003).
[5] P. L. McEuen, IEEE Trans. Nanotechnol. **1**, 78 (2002).
[6] R. Martel *et al.*, Phys. Rev. Lett. **87**, 256805 (2001).
[7] M. Radosavljevic *et al.*, Appl. Phys. Lett. **83**, 2435 (2003).
[8] J. A. Misewich *et al.*, Science **300**, 783 (2003).
[9] S. Huang *et al.*, Adv. Mater. **15**, 1651 (2003); S. Huang, X. Cai, and J. Liu, J. Am. Chem. Soc. **125**, 5636 (2003).
[10] J. Guo, S. Datta, and M. Lundstrom, IEEE Trans. Electron Devices **51**, 172 (2004).
[11] M. S. Fuhrer *et al.*, Nano Lett. **2**, 755 (2002).
[12] M. Radosavljevic *et al.*, Nano Lett. **2**, 761 (2002).
[13] M. Freitag *et al.*, Nano Lett. **4**, 1063 (2004).
[14] Z. Yao, C. L. Kane, and C. Dekker, Phys. Rev. Lett. **84**, 2941 (2000).
[15] M. Freitag *et al.*, Phys. Rev. Lett. **89**, 216801 (2001).
[16] M. P. Anantram, Phys. Rev. B **62**, R4837 (2000).